

MSUHEP-10615
July 6, 2001
hep-ph/0106181

Review of BFKL

CARL R. SCHMIDT*

*Department of Physics and Astronomy
Michigan State University, East Lansing, MI 48824 USA*

I describe the underlying physics behind the BFKL resummation and discuss some of the recent ideas and results in this field. On the theoretical side I consider the formalism in the next-to-leading logarithmic (NLL) approximation and the interpretation of the large corrections. On the phenomenological side I discuss several experiments that attempt to observe the BFKL effects in the high energy limit.

Presented at the

5th International Symposium on Radiative Corrections
(RADCOR-2000)

Carmel CA, USA, 11–15 September, 2000

*Work supported by the US National Science Foundation under grants PHY-9722144 and PHY-0070443.

1 Introduction to BFKL

Hadronic processes at high-energy colliders often involve more than one energy scale. As a consequence, calculations in perturbative Quantum Chromodynamics (QCD) can involve large logarithms of the ratio of these scales, which must be resummed to obtain a reliable prediction. Two processes where this might be necessary are Deep Inelastic Scattering (DIS) at small x and hadronic dijet production at large rapidity intervals Δy . In DIS the logarithm that appears is $\ln(1/x)$, with $x \simeq Q^2/s$ the squared ratio of the momentum transfer to the photon-hadron center-of-mass energy. In large-rapidity dijet production the large logarithm is $\Delta y \simeq \ln(\hat{s}/|\hat{t}|)$, with \hat{s} the squared parton center-of-mass energy and $|\hat{t}|$ of the order of the squared jet transverse energy. In both of these cases the large logarithms, which arise at each order in the coupling constant α_s , can be resummed by means of the Balitsky-Fadin-Kuraev-Lipatov (BFKL) equation [1].

The most familiar prediction of the BFKL resummation in the leading logarithmic (LL) approximation is the power-law rise in the partonic cross section as a function of the energy:

$$\hat{\sigma} \approx e^{A\Delta y} \approx \hat{s}^A. \quad (1)$$

The quantity $(1 + A)$ is often referred to as the BFKL Pomeron intercept, where at LL

$$A = \bar{\alpha}_s 4 \ln 2 \quad (2)$$

with $\bar{\alpha}_s = N_c \alpha_s / \pi$ and $N_c = 3$ the number of colors. Similarly, in DIS the structure functions are predicted to rise as x^{-A} at small x . One of the goals in BFKL physics has been to observe this power-law rise as a direct indication of the importance of the resummation. In this talk I will review the status of BFKL physics, both in its theoretical development at next-to-leading logarithm (NLL) and in its phenomenological application to experiment.

2 BFKL at LL

I begin by giving a simple physical picture of the BFKL resummation at leading logarithm (LL), where the large logarithm is taken to be the rapidity interval between two widely-separated partonic jets. Although this in no way can be considered a derivation of the BFKL equation, it is useful to show what assumptions go into the resummation and to show how the factors of $\alpha_s \Delta y$ arise at each order and exponentiate.

The starting point is the factorization of the partonic cross section at large rapidity separation:

$$\frac{d\hat{\sigma}}{d^2 p_{a\perp} d^2 p_{b\perp}} = V_a(p_{a\perp}^2) f(\Delta y, p_{a\perp}, p_{b\perp}) V_b(p_{b\perp}^2). \quad (3)$$

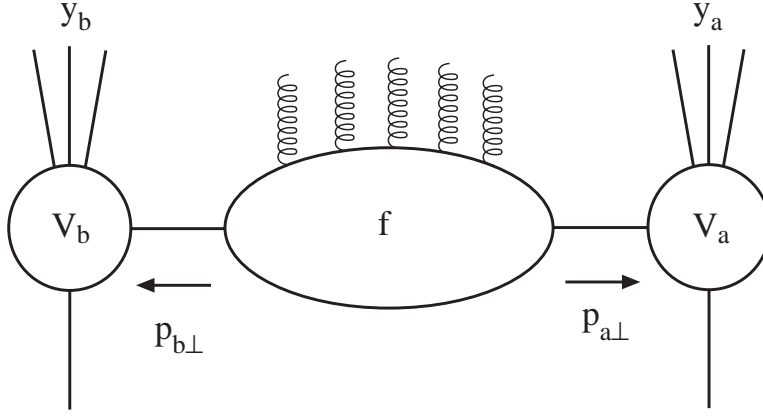


Figure 1: A schematic picture of the cross section for producing particles at large rapidity separation.

A physical interpretation of this factorization is represented in Fig. 1. The process consists of two distinct scatterings, which occur at widely-separated rapidities, y_a and y_b , and small transverse momenta $|p_{a\perp}| \sim |p_{b\perp}|$. The impact factors $V(p_\perp^2)$ depend only on the transverse momentum exchanged and the specific partons involved in each scattering, but not on anything else that happens in the event. The function $f(\Delta y, p_{a\perp}, p_{b\perp})$ connects the two scatterings by accounting for the emission of gluons in the rapidity interval. This function is universal and provides the exponentiation of the logarithms.

We can see this factorization directly in the Born cross section for gluon-gluon scattering at $y_a \gg y_b$, shown diagrammatically in Fig. 2(a):

$$\frac{d\hat{\sigma}_{gg}^{(0)}}{d^2p_{a\perp}d^2p_{b\perp}} = \left[\frac{N_c\alpha_s}{p_{a\perp}^2} \right] \left[\frac{1}{2}\delta^{(2)}(p_{a\perp} + p_{b\perp}) \right] \left[\frac{N_c\alpha_s}{p_{b\perp}^2} \right], \quad (4)$$

where the central factor is the $\mathcal{O}(\alpha_s^0)$ contribution to the function f , and we see that the leading-order gluon impact factor is

$$V_g(p_\perp^2) = \frac{N_c\alpha_s}{p_\perp^2}. \quad (5)$$

The real $\mathcal{O}(\alpha_s^1)$ correction to f can be obtained by considering the emission of three gluons, strongly ordered in rapidity $y_a \gg y_1 \gg y_b$, shown diagrammatically in Fig. 2(b):

$$\frac{d\hat{\sigma}_{gg}^{(1r)}}{d^2p_{a\perp}d^2p_{b\perp}} = \left[\frac{N_c\alpha_s}{p_{a\perp}^2} \right] \left[\frac{\bar{\alpha}_s}{\pi} \int \frac{d^2k_{1\perp}dy_1}{k_{1\perp}^2} \frac{1}{2}\delta^{(2)}(p_{a\perp} + k_{1\perp} + p_{b\perp}) \right] \left[\frac{N_c\alpha_s}{p_{b\perp}^2} \right]. \quad (6)$$

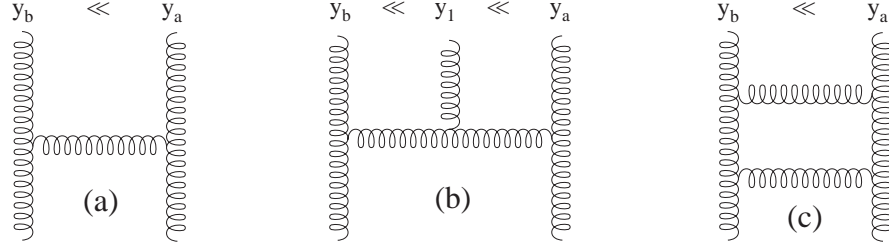


Figure 2: Contributions to LL BFKL ladder obtained from gg scattering: (a) $(\alpha_s \Delta y)^0$ real. (b) $(\alpha_s \Delta y)^1$ real. (c) $(\alpha_s \Delta y)^1$ virtual.

From this formula, we easily see where the large logarithm comes from. It arises from the integral over the rapidity y_1 of the intermediate gluon, resulting in a factor of $\alpha_s \Delta y$.

We can now generalize the form of these real corrections to an arbitrary number of emitted gluons:

- At each order, another gluon is inserted in the ladder with a weight given by

$$\frac{\bar{\alpha}_s}{\pi} \frac{d^2 k_{i\perp}}{k_{i\perp}^2} .$$

- The emitted gluons conserve transverse momentum, as enforced by a delta-function factor

$$\frac{1}{2} \delta^{(2)}(p_{a\perp} + \sum_i k_{i\perp} + p_{b\perp}) .$$

- The intermediate gluons are integrated over the ordered rapidity-intervals,

$$y_b < y_1 < y_2 < \cdots < y_n < y_a ,$$

producing an overall factor of

$$\frac{(\Delta y)^n}{n!} .$$

The real n -gluon contribution can be obtained directly from the tree-level $(n+2)$ -gluon cross-section by assuming that all transverse momenta are comparable in size, while terms suppressed by $\mathcal{O}(e^{-|y_i - y_j|})$ are neglected.

Of course, the real contributions by themselves are not infrared-safe, because they diverge when the k_\perp of any of the intermediate gluons vanishes. The cure for this is the inclusion of virtual corrections in the large Δy limit. The $\mathcal{O}(\alpha_s^1)$ virtual correction

in gg scattering comes from the diagram in Fig. 2(c). Similar contributions must come in at each order to regularize the $1/k_\perp^2$ infrared singularities. Including these corrections, we can understand the following form of the BFKL equation

$$\begin{aligned}
f(\Delta y, p_{a\perp}, p_{b\perp}) &= \frac{1}{2} \delta^{(2)}(p_{a\perp} + p_{b\perp}) \\
&+ (\Delta y) K \left[\frac{1}{2} \delta^{(2)}(p_{a\perp} + p_{b\perp}) \right] \\
&+ \frac{1}{2!} (\Delta y)^2 K \left[K \left[\frac{1}{2} \delta^{(2)}(p_{a\perp} + p_{b\perp}) \right] \right] \\
&+ \frac{1}{3!} (\Delta y)^3 K \left[K \left[K \left[\frac{1}{2} \delta^{(2)}(p_{a\perp} + p_{b\perp}) \right] \right] \right] \\
&+ \dots, \tag{7}
\end{aligned}$$

where the kernel K is an integral operator acting on a function $\phi(p_{a\perp})$ by

$$K \left[\phi(p_{a\perp}) \right] = \frac{\bar{\alpha}_s}{\pi} \int \frac{d^2 k_\perp}{k_\perp^2} \left[\phi(k_\perp + p_{a\perp}) - \frac{p_{a\perp}^2}{k_\perp^2 + (k_\perp + p_{a\perp})^2} \phi(p_{a\perp}) \right]. \tag{8}$$

At LL, each operation of the kernel inserts one more real or virtual gluon in the ladder. The first term in (8) corresponds to a real gluon, while the second term is the virtual correction needed to regularize the soft singularity. The equation (7) is just the solution of the BFKL equation obtained by iteration.

A more compact form of the BFKL solution at LL is obtained by finding the eigenfunctions and eigenvalues of the kernel (8). This yields

$$f(\Delta y, p_{a\perp}, p_{b\perp}) = \frac{1}{i(2\pi)^2} \sum_{n=-\infty}^{\infty} e^{in\tilde{\phi}} \int_{1/2-i\infty}^{1/2+i\infty} d\gamma (p_{a\perp}^2)^{\gamma-1} (p_{b\perp}^2)^{-\gamma} e^{\bar{\alpha}_s \chi(n, \gamma) \Delta y}, \tag{9}$$

where $\tilde{\phi} = \phi_a - \phi_b - \pi$, the function

$$\bar{\alpha}_s \chi(n, \gamma) = \bar{\alpha}_s \left[2\psi(1) - \psi\left(\frac{n}{2} + \gamma\right) - \psi\left(\frac{n}{2} + 1 - \gamma\right) \right] \tag{10}$$

gives the eigenvalues of the LL BFKL kernel (8), and ψ is the logarithmic derivative of the gamma function. For very large Δy , the integral over γ in (9) can be performed in the saddle-point approximation. The $n = 0$ term dominates, and one obtains the exponential rise in the cross section (1), displayed in the introduction with $A = \bar{\alpha}_s \chi(0, \frac{1}{2}) = 4\bar{\alpha}_s \ln 2$.

3 BFKL at NLL

At LL each application of the kernel gives a contribution of $\mathcal{O}(\alpha_s \Delta y)$. At NLL one also includes terms of $\mathcal{O}(\alpha_s^2 \Delta y)$. That is, we can reinterpret the kernel in (7) as a

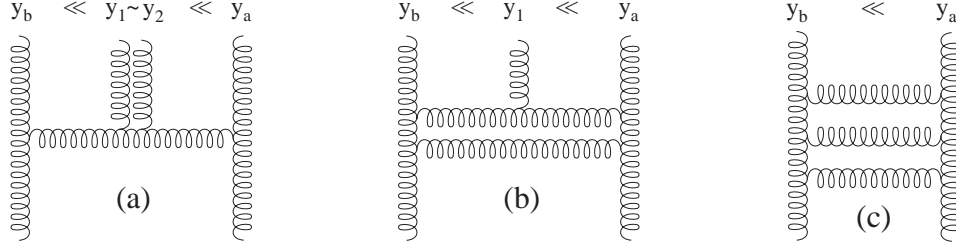


Figure 3: Contributions to NLL BFKL ladder at $\mathcal{O}(\alpha_s^2 \Delta y)$ obtained from gg scattering.

power series $K \equiv \bar{\alpha}_s K^{(1)} + \bar{\alpha}_s^2 K^{(2)} + \dots$, where $\bar{\alpha}_s K^{(1)}$ is the LL kernel, given in (8), and $\bar{\alpha}_s^2 K^{(2)}$ includes the NLL corrections. There are three types of contributions at NLL, which are shown schematically, in the context of gg scattering, in Fig. 3. They consist of: (a) the emission of two gluons nearby in rapidity, (b) the virtual correction to the emission of one gluon, widely separated in rapidity, (c) the subleading purely-virtual corrections. These three types of contributions took many years and many papers to sort out the technical details¹, with the final NLL kernel obtained in 1998 by Fadin and Lipatov [3]. Although the full kernel has not been checked in a completely independent manner, many of the pieces of the calculation have received independent confirmation. Two particularly significant checks are the calculation of the virtual correction to the gluon emission at large rapidity separation [4], and the compilation of the three NLL terms into a single kernel with the cancellation of all collinear and soft singularities [5].

The final result of this calculation is usually presented by applying the NLL kernel to the LL eigenfunctions, with azimuthal averaging, yielding

$$\begin{aligned}
 K_{\text{NLL}} \left[(p_{a\perp}^2)^{\gamma-1} \right] &= \left\{ \bar{\alpha}_s(\mu) \chi(\gamma) \right\} (p_{a\perp}^2)^{\gamma-1} \\
 &= \left\{ \bar{\alpha}_s(\mu) \chi^{(1)}(\gamma) \left[1 - \bar{\alpha}_s(\mu) b_0 \ln(p_{a\perp}^2/\mu^2) \right] \right. \\
 &\quad \left. + \bar{\alpha}_s(\mu)^2 \chi^{(2)}(\gamma) \right\} (p_{a\perp}^2)^{\gamma-1}
 \end{aligned} \tag{11}$$

where $\bar{\alpha}_s \chi^{(1)}(\gamma)$ is the LL eigenvalue for $n = 0$ given in (10), $b_0 = 11/12 - n_f/(6N_c)$, and we have explicitly included the dependence on the $\overline{\text{MS}}$ renormalization scale μ . The NLL correction has been separated into two terms. The first term depends on the scale $p_{a\perp}$ and is associated with the running of the coupling in the LL kernel: $\alpha_s(\mu) \rightarrow \alpha_s(p_{a\perp})$. The second term, $\bar{\alpha}_s^2 \chi^{(2)}(\gamma)$, is independent of scale and contains the remainder of the NLL corrections [3].

After completion of the NLL corrections to the BFKL kernel, several issues quickly became apparent. Roughly speaking, they can be separated into issues associated

¹A list of references can be found in ref. [2], but with no guarantee of completeness.

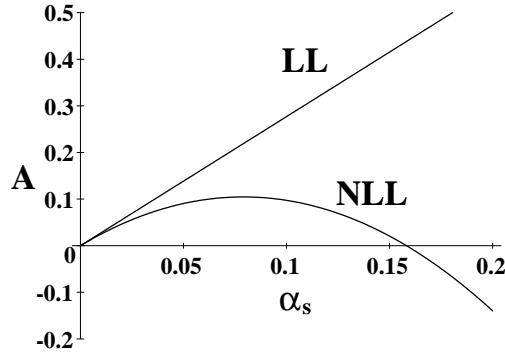


Figure 4: Leading BFKL eigenvalue $A = \bar{\alpha}_s \chi(\frac{1}{2})$ at LL and NLL.

with the running coupling term and issues associated with the scale-invariant term. In this talk I will concentrate on the scale-invariant term. For analyses of the running coupling issues, see Refs. [6–9].

The first indication of problems with BFKL at NLL was seen immediately by Fadin and Lipatov. The corrections to the leading eigenvalue are large and negative! If we ignore the effects of running coupling, we obtain

$$\bar{\alpha}_s \chi(\frac{1}{2}) = 2.77\bar{\alpha}_s - 18.34\bar{\alpha}_s^2, \quad (12)$$

for three active flavors. This function is plotted in Fig. 4. At the not-unreasonable value of $\alpha_s = 0.16$ the NLL corrections exactly cancel the LL term, while for larger values of α_s the eigenvalue becomes negative. Naively, this would indicate that the BFKL Pomeron intercept also becomes negative, leading to a cross section that decreases, rather than increases, as a power of the energy.

Unfortunately, things get even worse. The standard BFKL power-law scaling of the partonic cross section (1) relies on the saddle-point evaluation of the NLL generalization of the BFKL solution (9). Upon closer analysis Ross [10] showed that the NLL eigenvalue function $\chi(\gamma)$ no longer has a maximum at $\gamma = \frac{1}{2}$, but has a minimum with two maxima occurring symmetrically on either side of this point². Performing a higher-order expansion of $\chi(\gamma)$, Ross found a smaller correction to the BFKL Pomeron intercept. However, the cross section he obtained was not positive definite. It contained oscillations as one varied $p_{a\perp}$ and $p_{b\perp}$. This led Levin [8] to declare that NLL BFKL has a serious pathology.

²The standard procedure in these analyses is to modify the LL eigenfunctions used in eq. (11) in order to make the eigenvalues manifestly symmetric under $\gamma \rightarrow 1 - \gamma$, following ref. [3].

One might wonder whether the approximate evaluation of the integral performed by Ross is adequate at this stage. Perhaps an exact evaluation is necessary. However, negative cross sections have also arisen when the resummed small- x anomalous dimensions, obtained from the NLL BFKL solution, were used to study DIS scattering at small- x [11,12]. In any event the NLL corrections to the BFKL solution are large, leading one to question the stability and applicability of the BFKL resummation procedure in general.

4 Understanding the large NLL Corrections.

When any perturbation expansion has large corrections at higher orders, the natural thing to do is to try to reorganize the series so that it converges more rapidly. In this talk I will briefly discuss three different approaches to this reorganization.

The first proposal by Brodsky *et al.* [13] uses the freedom to choose the renormalization scheme. The NLL eigenvalue equation (12) is written in the $\overline{\text{MS}}$ scheme. Brodsky *et al.* argued that a non-abelian physical scheme should be more natural for the BFKL resummation. Then they used the BLM procedure [14] to find the optimal scale for the QCD coupling. In this case the BLM procedure dictates a large scale, thereby reducing the effective α_s (and the LL prediction) and also reducing the coefficient of the NLL α_s^2 term. This approach predicts a BFKL Pomeron intercept of $A \sim 0.17$ for $\alpha_s = 0.2$. In addition it yields a very weak dependence on the gluon virtuality $p_{a\perp}^2$ and leads to an approximate conformal invariance.

The motivation for the second proposal [2] (first suggested in [15] and [16]) can be seen from the discussion of the physics of BFKL at LL in section 2. The approximation used in deriving the LL contribution at each order in the BFKL ladder was to neglect terms of $\mathcal{O}(e^{-|y_i - y_{i+1}|})$ in the QCD matrix elements, which is valid when the emitted gluons are all widely separated in rapidity. However, the gluon rapidity y_i is then integrated all the way up to y_{i+1} . Thus, the errors in the matrix elements are largest when $y_i \sim y_{i+1}$. This suggests that one enforce a condition $y_{i+1} - y_i > \Delta$, so that the gluons are required to be widely separated, and the kinematic approximations are good. The arbitrary parameter Δ is assumed to be much smaller than the total rapidity interval. The excluded region is re-introduced at NLL, such that the change in the cross section due to shifting Δ is always next-to-next-to-leading logarithm (NNLL). In this way, the dependence on Δ can be regarded as an estimate of the uncertainty due to NNLL corrections (similar to the role of the renormalization scale μ in the $\overline{\text{MS}}$ scheme).

Fig. 5 shows the dependence on Δ of the leading eigenvalue and its second derivative at LL and NLL for $\alpha_s = 0.15$ in this modified BFKL theory. Note that the corrections to $\bar{\alpha}_s \chi(\frac{1}{2})$ are not large for $\Delta \gtrsim 2$ and have weak dependence on Δ for large Δ . Also, the point $\gamma = \frac{1}{2}$ is a maximum for this coupling as long as $\Delta \gtrsim 2.2$.

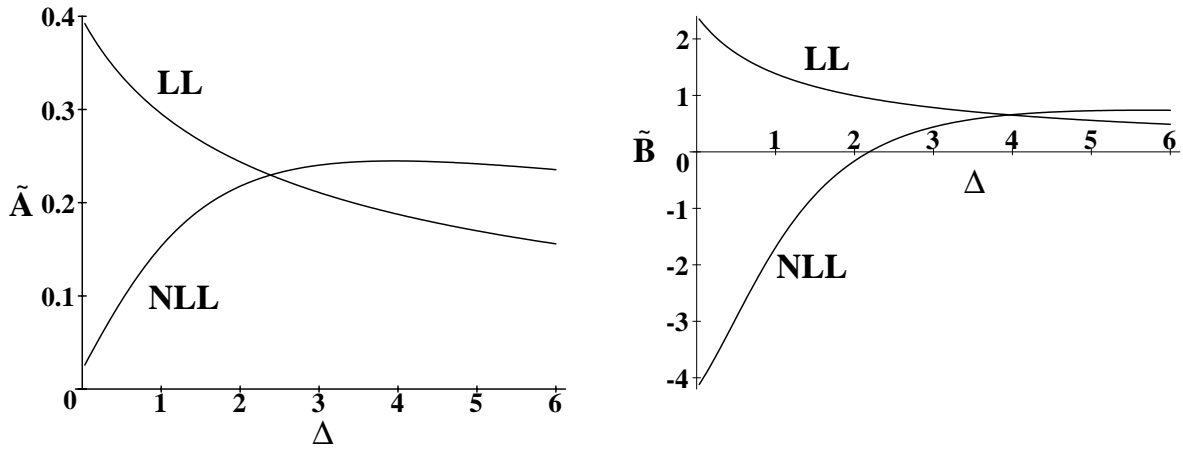


Figure 5: Dependence of $\tilde{A} = \bar{\alpha}_s \chi(\frac{1}{2})$ and $\tilde{B} = -\frac{1}{2} \bar{\alpha}_s \chi''(\frac{1}{2})$ on Δ for $\alpha_s = 0.15$, from Ref. [2].

Thus, the BFKL resummation is stable for large enough Δ . This modification of the BFKL resummation predicts a somewhat larger value of the BFKL pomeron intercept than the previous proposal. However, the implications of a large value of Δ for the phenomenological use of BFKL is open to interpretation.

The third and perhaps most ambitious proposal [17,9] to control the large NLL corrections is to systematically include the largest collinearly-enhanced, but still sub-leading corrections into LL BFKL. The most important of these are energy-scale corrections [5]. To understand the origin of these corrections, note that in our discussion of BFKL at LL in section 2 we chose to work with the symmetric rapidity $\Delta y = \ln \hat{s}/(p_{a\perp} p_{b\perp})$ as the large logarithm to resum. However, we could equally well have chosen $y^+ = \ln x_a^+/x_b^+ = \ln \hat{s}/p_b^2$ or $y^- = \ln x_b^-/x_a^- = \ln \hat{s}/p_a^2$, where x_i^\pm is the momentum fraction along the positive or negative light-cone for the emitted gluon i . These choices are all equivalent at LL because the transverse momenta are treated as comparable in size; however, at NLL they are inequivalent. A change in the logarithm produces a change in the NLL kernel and can introduce double transverse logarithms of the form $\bar{\alpha}_s \ln^2(p_{a\perp}^2/p_{b\perp}^2)$ into the resummation.

Motivated by DGLAP-type resummation [18] one finds that the appropriate choice is to resum y^+ when $p_{b\perp}^2 \gg p_{a\perp}^2$ and y^- when $p_{a\perp}^2 \gg p_{b\perp}^2$. The effect of these changes of the BFKL resummation variable was studied in refs. [5] and [3], and the corresponding terms in the NLL eigenvalue $\chi^{(2)}(\gamma)$ were isolated and resummed in ref. [17]. Additional collinearly-enhanced terms due to the effects of the running coupling and the non-singular part of the splitting functions have also been considered

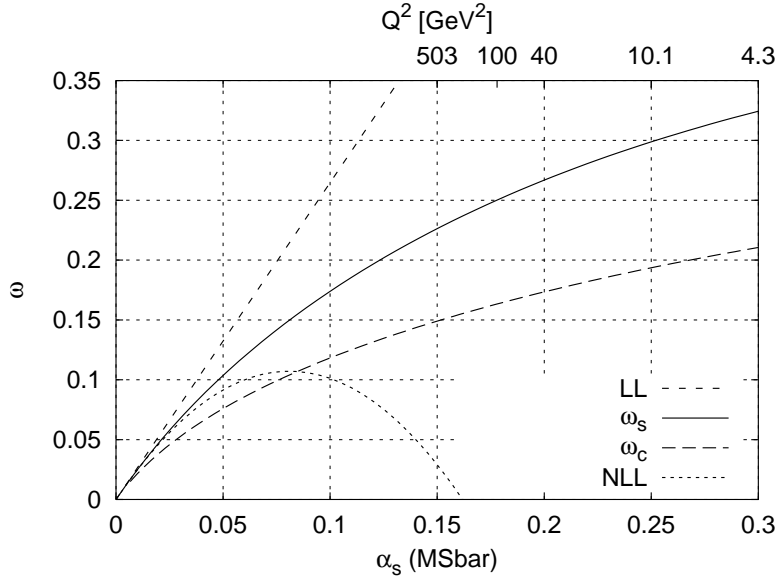


Figure 6: The BFKL Pomeron intercept (here labeled ω) at LL, NLL and with the collinearly-enhanced resummation included at NLL, from Ref. [9]. The curve ω_s corresponds to the coefficient for the exponential rise in Δy , which is what we have focused on in this talk. The curve ω_c corresponds to the power growth of the small- x splitting functions. Although identical in LL BFKL, these two coefficients differ at NLL.

and resummed in Ref. [9]. A nice discussion of these ideas can be found in ref. [19].

A similar approach, advocated in Refs. [20], is to use the “duality” relations between the BFKL $\ln(1/x)$ and the DGLAP $\ln(Q^2)$ resummations to incorporate the dominant collinear effects into BFKL at small x . Adding contributions obtained from the known LO and NLO DGLAP anomalous dimensions, one gets a “double leading” expansion for the BFKL function $\chi(\gamma)$, which is better behaved and more stable in the collinear region near $\gamma = 0$.

Results of the collinearly-enhanced resummation from Ref.[9] are shown in Fig. 6, where the leading eigenvalue $\omega_s = \bar{\alpha}_s \chi(\frac{1}{2})$ is plotted as a function of $\bar{\alpha}_s$. As in the other cases the eigenvalue is found to be positive after resummation, yielding a value of about $\omega_s = 0.27$ for $\alpha_s = 0.2$. In addition the characteristic eigenvalue function of γ is stable for values of α_s of interest.

The physical implications of the energy-scale dependence can be seen by further investigating the relation between resummation in y^\pm and Δy . When $p_{b\perp}^2 \gg p_{a\perp}^2$, the resummation in y^+ requires the ordering $x_a^+ > x_b^+$. Translating back into the symmetric variable, this implies $\Delta y > \ln(p_{b\perp}/p_{a\perp})$. Similarly, when $p_{a\perp}^2 \gg p_{b\perp}^2$, the resummation in y^- requires the ordering $x_b^- > x_a^-$, implying $\Delta y > \ln(p_{a\perp}/p_{b\perp})$. These constraints hold for any two successively emitted gluons. Therefore, the incorporation of these collinear effects corresponds to imposing a p_\perp -dependent cut, $y_{i+1} - y_i >$

$|\ln(p_{i\perp}/p_{i+1\perp})|$, on the separation in rapidity between the neighboring gluons. Since this cut is very similar to the rapidity veto of proposal two, it is understandable that when both the collinear resummation and the rapidity veto are included, as studied in Ref. [21], the dependence on the parameter Δ was significantly reduced, even for small Δ .

5 Phenomenology of BFKL

Although the theoretical studies of BFKL have been focused on its behavior at NLL, the level of most phenomenological studies is still at LL. To treat a process consistently at NLL, one also must incorporate the $\mathcal{O}(\alpha_s)$ corrections to the impact factors. Although these corrections are known for some processes, at least at the amplitude level, they have yet to be incorporated into a consistent calculation suitable for phenomenological studies.

In this section I will discuss several probes of BFKL physics in hadron-hadron, lepton-hadron, and $\gamma^*\gamma^*$ collisions. I will only consider processes for which the relevant transverse scales $p_{a\perp}, p_{b\perp}$ on both sides of the BFKL ladder can be considered perturbative. In particular, I will not consider the inclusive $F_2(x, Q^2)$ in DIS, because it is necessarily dependent on non-perturbative inputs.

5.1 BFKL probes at the Tevatron

One of the most thoroughly studied searches for BFKL physics has been by the DØ collaboration in $p\bar{p}$ collisions at the Fermilab Tevatron. As in all BFKL experimental studies, the basic idea is to analyze the events in a configuration which most closely approximates that used in the BFKL resummation. Jets, with transverse momentum above some $E_{\perp\min}$, are tagged and ordered in rapidity. Then one defines observables as a function of $\Delta y = y_a - y_b$, where y_a and y_b are the rapidities of the most forward and backward jets, respectively.

The most natural BFKL signal would be the power-law growth in the partonic cross section with Δy , as in Eq. (1). However, at fixed center-of-mass energy this growth is swamped by the effects of steeply falling parton distribution functions (PDFs) which are relevant when far forward or backward jets are produced. Thus, the first observable to be considered was the decorrelation in azimuthal angle between the two tagged jets as a function of Δy . Physically, this effect is easy to understand. In the Born approximation, only two jets are produced, and by momentum conservation they must be back-to-back. However, as the rapidity interval increases, there is more room for additional jets, and the tagged jets become decorrelated. This can be seen directly in the BFKL solution (9). At small Δy , all terms in the Fourier series in $\tilde{\phi} = \phi_a - \phi_b - \pi$ are approximately equal, producing a delta-function in $\tilde{\phi}$ which forces the two jets to be back to back. As Δy increases, the higher order terms

become smaller and smaller compared to the leading $n = 0$ term, so the jets become completely decorrelated [22]. The simplest observable to display this effect is the moment $\langle \cos \tilde{\phi} \rangle$, which goes to 1 if the jet azimuthal angles are completely correlated and goes to 0 if they are completely decorrelated [23].

Even before the DØ analysis was completed, however, it was realized that there was a serious problem in using LL BFKL for phenomenological analyses at hadron colliders: the BFKL resummation includes the contribution of energetically disfavored or disallowed configurations in its predictions. In principle these configurations are subleading, but in practice they are very important [24]. (In fact these effects could be considered to be a foreshadowing of the large corrections to BFKL at NLL.) We can understand this effect by considering the Feynman x -values used in the PDFs. The exact values are given by conservation of light-cone momentum along the beam axis and can be written

$$\begin{aligned} x_a &= \frac{1}{\sqrt{s}} \left(p_{a\perp} e^{y_a} + p_{b\perp} e^{y_b} + \sum_i k_{i\perp} e^{y_i} \right) \\ x_b &= \frac{1}{\sqrt{s}} \left(p_{a\perp} e^{-y_a} + p_{b\perp} e^{-y_b} + \sum_i k_{i\perp} e^{-y_i} \right), \end{aligned} \quad (13)$$

where the sum is over all partons produced in the event. In the “naive” LL BFKL one only keeps the leading contributions,

$$\begin{aligned} x_a^0 &= \frac{p_{a\perp} e^{y_a}}{\sqrt{s}} \\ x_b^0 &= \frac{p_{b\perp} e^{-y_b}}{\sqrt{s}}. \end{aligned} \quad (14)$$

That is, one convolutes the analytic LL BFKL solution (9) with the impact factors, using the PDFs evaluated at $x_{a,b}^0$. However, the true $x_{a,b}$ are always larger than $x_{a,b}^0$, and the energy-momentum constraints $x_{a,b} < 1$ are not enforced in the naive BFKL calculation. If the PDFs vary strongly with x , this can greatly overestimate the contributions from multi-jet events.

With the analytic LL BFKL solution (9) the phase space of the intermediate gluons has already been integrated over, so there is no choice but to use the leading x^0 's (14) in the PDFs. However, in a BFKL Monte Carlo solution [25,26] one generates the gluon ladder directly as in Eq. (7). Thus, one has information on all the produced partons, and one can enforce energy conservation on the solution by using the exact x 's (13) in the PDFs. This greatly improves the reliability of the BFKL prediction.

In Fig. 7 we show the DØ azimuthal decorrelation data from Ref. [27] compared with the naive LL BFKL and a Monte Carlo BFKL calculation with energy conservation included. The data shows $\langle \cos \tilde{\phi} \rangle$ as a function of Δy at $\sqrt{s} = 1.8$ TeV, where the tagging jets are required to have $E_\perp > 20$ GeV. The naive BFKL severely

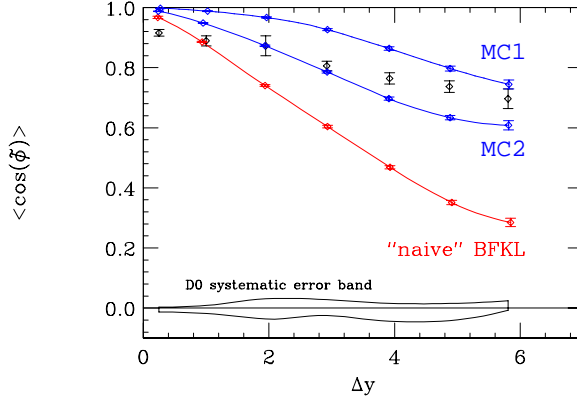


Figure 7: Azimuthal angle decorrelation as a function of rapidity interval. The DØ data is from [27], the lowest curve is “naive” BFKL, the two upper curves are BFKL Monte Carlo predictions. The correlated systematic error is due to jet energy scale uncertainty.

overestimates the rate of decorrelation with Δy , due to the overweighting of energetically disfavored or disallowed configurations. The two BFKL Monte Carlo curves are produced by the Monte Carlo in Ref. [25]. Both use the exact x ’s in the PDFs, but use different approximations to relate the partonic to the hadronic cross sections in the high energy limit. The difference between the two approximations is subleading in the high energy limit. The BFKL Monte Carlo with energy conservation certainly works much better than the naive BFKL, but the subleading uncertainties are still sizeable, as displayed by the difference between the two Monte Carlo predictions.

An argument against the decorrelation measurement as a signal of BFKL is that it probes the region around $\tilde{\phi} \approx 0$, which is also most sensitive to Sudakov logarithms. It would be nicer to probe directly the rise in partonic cross section with the partonic energy as in Eq. (1). This became possible when the Tevatron collider was run at the lower energy of 630 GeV, allowing a comparison of dijet production at two different center-of-mass energies. By binning the events in the partonic x_a, x_b values rather than in Δy , the dependence on the PDFs should cancel in the ratio

$$R = \frac{\sigma(\sqrt{s_1} = 1800\text{GeV})}{\sigma(\sqrt{s_2} = 630\text{GeV})} . \quad (15)$$

This is the original proposal of Mueller and Navelet [28]. Using the asymptotic saddle point approximation, one obtains a prediction of

$$R_{\text{BFKL}} = \frac{e^{A(\Delta y_1 - \Delta y_2)}}{\sqrt{\Delta y_1 / \Delta y_2}} , \quad (16)$$

where $\Delta y_i \approx \ln(\hat{s}_i / p_{a\perp} p_{b\perp}) \approx \ln(\hat{s}_i / E_{\perp\text{min}}^2)$. This ratio was measured by the DØ collaboration, in several x bins, with the following cuts: $E_{\perp\text{min}} > 20$ GeV, $|y| < 3$,

$\Delta y > 2$, and $400 < Q^2 = E_{a\perp} E_{b\perp} < 1000 \text{ GeV}^2$. Using the formula (16), a BFKL Pomeron intercept of $A = 0.65 \pm 0.07$ was extracted [29].

This measurement is noteworthy in that it is probably the only current measurement which shows a rise in the cross section that is *larger* than the LL BFKL prediction. Using $\alpha_s(20 \text{ GeV}) = 0.17$ in Eq. (2), one obtains a LL prediction of $A = 0.45$, which is almost 3 standard deviations below the extracted value. However, as discussed in Ref. [30], one must be careful in interpreting this measurement. First, the extraction of the BFKL Pomeron intercept from (16) assumes that the asymptotic BFKL expression is valid, and the experimental cuts and precise definition of the x 's do not significantly affect the asymptotics. In particular the cut on Q^2 was seen to slow the approach to asymptotics, resulting in a smaller predicted value for the ratio R . The inclusion of energy conservation via a BFKL Monte Carlo further reduced the predicted ratio. Finally, it was shown that the use of equal E_\perp cuts on both of the tagging jets introduces the same large Sudakov logarithms that plague the decorrelation measurement. Thus, it seems unlikely that the large ratio found by the DØ collaboration can be attributed to perturbative BFKL.

5.2 BFKL probes at HERA

It is also possible to look for the BFKL rise in the cross section in deep inelastic scattering (DIS) by tagging a forward jet [31,32]. Referring to the high energy factorization picture of Fig. 1, the DIS setup consists of the scattering of an off-shell photon with virtuality Q^2 and Bjorken $x_{bj} = Q^2/s_{ep}$ on the left, the scattering of a forward jet of momentum fraction $x_{jet} = E_{jet}/E_p$ and transverse momentum p_\perp on the right, connected by the BFKL ladder of gluon emissions in the middle. If $Q^2 \sim p_\perp^2 \gg \Lambda_{QCD}^2$, then the BFKL evolution is perturbative. The large logarithm that is resummed is $\ln(x_{jet}/x_{bj})$.

This DIS setup has several advantages over the $p\bar{p}$ setup, due to its asymmetric nature. Note that in the high energy limit, the PDF of the proton is evaluated at x_{jet} . Thus, with x_{jet} fixed, one can vary the rapidity interval at a single collider energy by varying x_{bj} , without any change in the PDF. In addition, this suggests that the energy conservation effects mentioned above may be less important, or at least not so strongly dependent on x_{bj} . Finally, the resummation in $\ln(x_{jet}/x_{bj})$, rather than in the jet rapidity intervals, is more natural here, and perhaps more stable theoretically, since it corresponds to the standard DGLAP evolution variable when $Q^2 > p_\perp^2$. The only major disadvantage is that the virtual photon impact factor is more complicated theoretically than the gluon or quark impact factors. Indeed, it has not been calculated completely at NLO.

Both the H1 [33] and ZEUS [34] collaborations have measured this forward jet cross section. The main experimental cuts on the forward jet itself are $x_{jet} > 0.035$, $E_{\perp jet} > 3.5$ and 5 GeV for H1, $x_{jet} > 0.036$, $E_{\perp jet} > 5$ GeV for ZEUS, and $0.5 < E_{\perp jet}^2/Q^2 < 2$ for both. The H1 data is displayed in Fig. 8. In Figs. 8(a) and (c) the

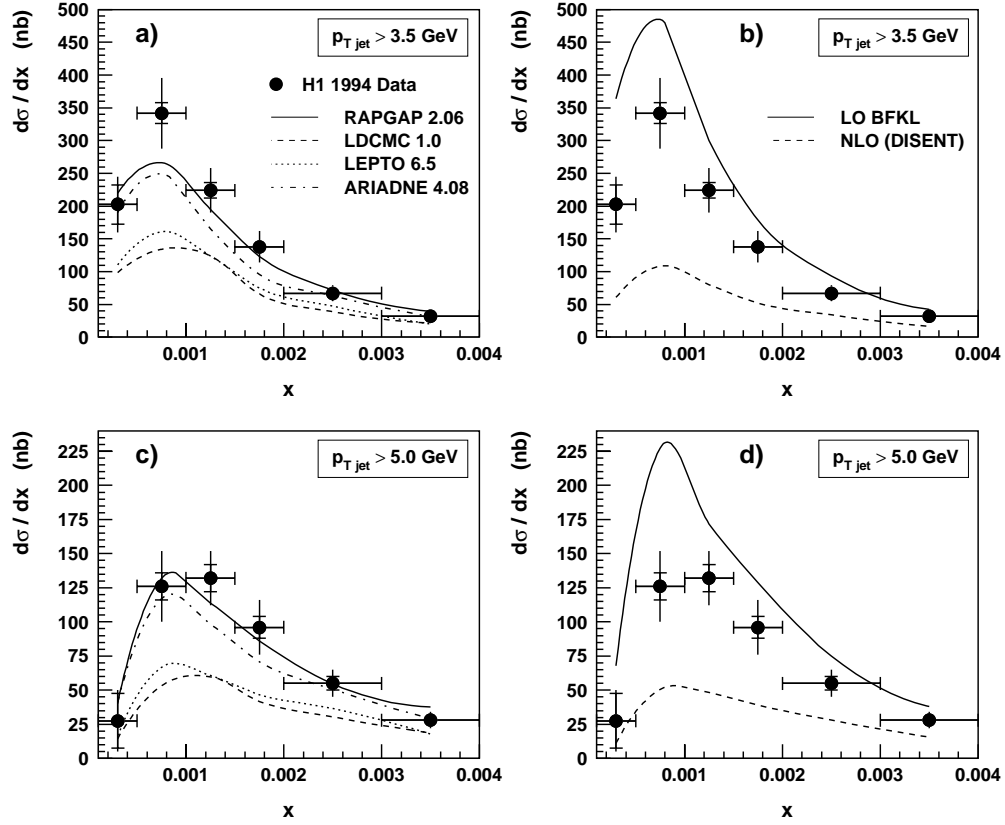


Figure 8: Forward jet cross-sections as a function of Bjorken- x from H1 [33] for two p_{\perp} cuts of 3.5 and 5 GeV. The data in (a) and (c) are compared with Monte-Carlo model predictions, including hadronization. The data in (b) and (d) are compared with partonic NLO $\mathcal{O}(\alpha_s^2)$ and LL BFKL calculations.

data is compared against several hadron-level Monte Carlo shower models attached to lowest order QCD matrix elements. The two that agree the best with the data are ARIADNE [35] and RAPGAP [36]. ARIADNE is based on the colour dipole model for gluon radiation which, like BFKL, lacks ordering in k_{\perp} . Gluon radiation in RAPGAP is based on DGLAP evolution, but this model also includes a resolved photon contribution to the basic QCD production mechanism. In Figs. 8(b) and (d) the H1 data is compared against a LL BFKL prediction [37] and a NLO QCD $\mathcal{O}(\alpha_s^2)$ prediction [38], both at the parton levels. The NLO calculation significantly underestimates the data at small x_{bj} , whereas the BFKL calculation overestimates it. This is not unreasonable, given that NLL corrections to BFKL are expected to reduce the rise at small x_{bj} , and that the kinematic cuts could not be included exactly in the calculation. The ZEUS data [34], shown in Fig. 9, similarly is far above a NLO

ZEUS 1995

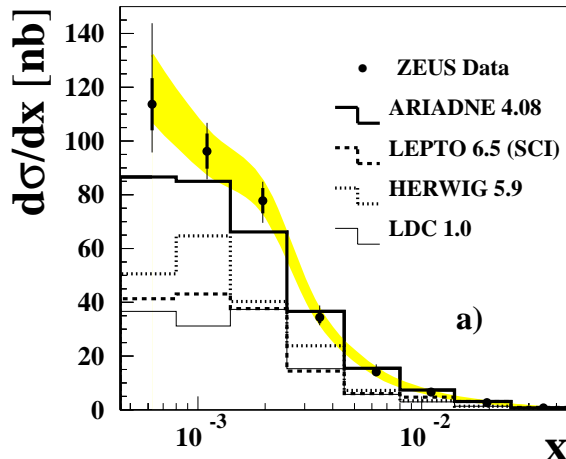


Figure 9: Forward jet cross-sections as a function of Bjorken- x from ZEUS [34] for $p_{\perp} > 5$ GeV. The data are compared with several Monte-Carlo model predictions at the hadron level.

QCD calculation [39], but below the LL BFKL expectations. A fit [40] to the data from both experiments using the LL BFKL cross section yielded an effective BFKL pomeron intercept corresponding to $A = 0.43 \pm 0.025(\text{stat}) \pm 0.025(\text{sys})$, compared to the LL prediction from Eq. (2) of $A = 0.75$ for $\alpha_s = 0.28$ at $Q^2 = 10 \text{ GeV}^2$.

Recently, several forward jet calculations with different approaches have shown good agreement with the data. One calculation [41] is based on LL BFKL, but modified by a consistency condition containing effects similar to the dominant NLL energy-scale effects discussed in section 4. A second calculation [42] is with a hadron-level Monte Carlo generator, based on the CCFM evolution [43], which is designed to agree with both DGLAP and BFKL in their respective regimes of reliability. Since both of these calculations can be considered LL BFKL, with some dominant subleading corrections included, this looks promising for BFKL. A third approach [44] which also fits the data is a NLO calculation that includes a resolved photon contribution, similar in spirit to the RAPGAP Monte Carlo. Interestingly, it appears that the success of this approach relies not on the evolution in Q^2 allowed by the inclusion of the photon PDF, but in the fact that it effectively approximates one term higher in α_s , via the NLO resolved piece. This is not incompatible with BFKL, since the new $\mathcal{O}(\alpha_s^3)$ contribution also includes the first gluon emission in the BFKL ladder. It is an interesting question to ask how the approximations in this picture of forward jet production mesh with those in the BFKL picture.

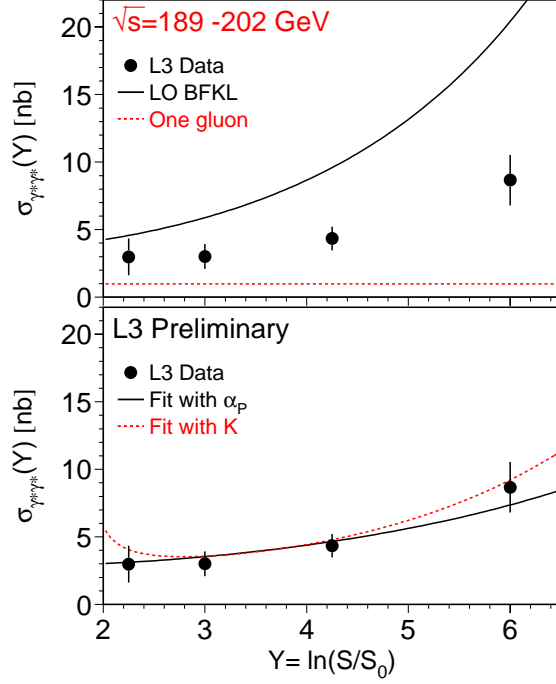


Figure 10: Two-photon cross-sections, $\sigma_{\gamma^*\gamma^*}$, after subtraction of the LO $\gamma^*\gamma^* \rightarrow q\bar{q}$ contribution at $\sqrt{s} \simeq 189 - 202 \text{ GeV}$ and $4 < Q_{1,2}^2 < 40 \text{ GeV}^2$, from Ref. [47]. The top figure compares the data with LO BFKL in the saddle point approximation with $A = \alpha_P - 1 = 0.53$ and with the one-gluon exchange diagram. The lower figure shows fits of the saddle-point BFKL expression to the data, allowing either α_P or the normalization K to vary.

5.3 BFKL probes in $\gamma^*\gamma^*$

Another standard BFKL measurement [45] is to observe the total $\gamma^*\gamma^*$ hadronic cross section as a function of $\sqrt{s_{\gamma\gamma}}$. This can be extracted from the process $e^+e^- \rightarrow e^+e^- + \text{hadrons}$ by tagging on the forward and backward electrons. In this case the two independent scatterings of Fig. 1 are the off-shell photons of momenta Q_1^2 and Q_2^2 that break up into color dipoles ($q\bar{q}$ pairs at leading order), which are then connected by the BFKL ladder. The large logarithm here is $Y \approx \ln(s_{\gamma\gamma}/\sqrt{Q_1^2 Q_2^2})$, in direct analogy to the hadron-hadron case.

This experiment has the advantage that, for large enough $Q_{1,2}^2$, there are no non-perturbative PDF inputs, so that in principle it is the cleanest probe, theoretically. However, from a purely calculational point of view, this process may be more complicated since it involves two off-shell photon impact factors. In particular, the cross-channel gluon on which the BFKL ladder is built does not even appear until NNLO in a standard perturbative QCD calculation..

The $\gamma^*\gamma^*$ hadronic cross section has been measured by the L3 [46,47] and the

OPAL [48] collaborations at LEP. In Fig. 10 we display the most recent preliminary L3 data [47]. The data clearly shows a rise with Y as expected by BFKL, but much less steep than LO BFKL. However, the data is above both LO and NLO QCD predictions [49]. In addition the data is also above the prediction from the single-gluon exchange contribution (evaluated using the average value of $\langle Q_{1,2}^2 \rangle = 15 \text{ GeV}^2$). In the lower figure the data is fitted to the asymptotic BFKL prediction

$$\sigma_{\gamma^*\gamma^*} = \frac{\sigma_0}{\sqrt{Q_1^2 Q_2^2 Y}} e^{AY}, \quad (17)$$

with either the overall normalization or the BFKL intercept $A = \alpha_P - 1$ left as a free parameter. The preliminary result in the latter case gives $A = 0.36 \pm 0.02$, which is more in line with NLO expectations. The OPAL preliminary measurements [48] give qualitatively similar results, but with less statistical significance.

6 Summary and Conclusions.

In this talk I have presented some recent results in BFKL physics, both in the theory and in its phenomenological applications. On the theoretical side, the focus has been on the large NLL corrections. At this time, it seems fairly safe to say that the original catastrophe of falling, or even negative, cross sections has been averted. By understanding the origin of these effects in the collinear behavior of the gluons, one can reorganize the resummation in order to move the dominant corrections back into the LL theory. Then the NLL prediction for the BFKL intercept is stable and slightly smaller than the standard LL prediction.

On the phenomenological side, the results look suggestive, especially in the DIS and $\gamma^*\gamma^*$ data. The cross sections are significantly above the state-of-the-art NLO QCD calculations, as they should be for a BFKL-enhanced observable. They are also in the range one might expect from a NLL BFKL calculation. However, the lesson learned from the analysis of the hadron-hadron experiments is that one must be very careful to consider how experimental cuts and kinematic effects, such as energy conservation, will affect these predictions. Although the asymmetric configuration of the DIS forward jet experiments and the lack of nonperturbative PDF-dependence in the $\gamma^*\gamma^*$ (assuming Q^2 is large enough) may make these observables less susceptible to large subleading effects, a thorough phenomenological analysis is certainly warranted.

With the completion and understanding of the NLL corrections to the BFKL kernel in hand, the next phase is to bring the phenomenological analyses up to the same NLL level. So far the major emphasis has been on the NLL BFKL intercept, but to make a full NLL prediction, with a reliable normalization, one also needs to combine this with NLO impact factors. In particular the NLO impact factor for the off-shell photon is crucial for the both the DIS and $\gamma^*\gamma^*$ analyses. In addition

the analyses must be performed in such a way as to treat the kinematics and cuts as accurately as possible. Promising steps in this direction are Refs. [41,17], which incorporate the largest NLL corrections into BFKL via a consistency condition, or via a CCFM Monte Carlo, respectively. Another useful exercise would be to incorporate the largest NLL corrections to the BFKL ladder into the BFKL Monte Carlos [25,26] and to modify them for use in the other experimental environments. This would be helpful for gauging the sensitivity to subleading kinematic effects (which arise at least as much from the impact factors as from the actual BFKL ladder). However, the greatest progress would come with a full NLL calculation with full NLO impact factors included. There is much work left to be done.

References

- [1] E. A. Kuraev, L. N. Lipatov and V. S. Fadin, Sov. Phys. JETP **44**, 443 (1976) [Zh. Eksp. Teor. Fiz. **71**, 840 (1976)];
E. A. Kuraev, L. N. Lipatov and V. S. Fadin, Sov. Phys. JETP **45**, 199 (1977) [Zh. Eksp. Teor. Fiz. **72**, 377 (1977)];
I. I. Balitsky and L. N. Lipatov, Sov. J. Nucl. Phys. **28**, 822 (1978) [Yad. Fiz. **28**, 1597 (1978)].
- [2] C. R. Schmidt, Phys. Rev. D **60**, 074003 (1999) [hep-ph/9901397].
- [3] V. S. Fadin and L. N. Lipatov, Phys. Lett. B **429**, 127 (1998) [hep-ph/9802290].
- [4] V. Del Duca and C. R. Schmidt, Phys. Rev. D **59**, 074004 (1999) [hep-ph/9810215].
- [5] G. Camici and M. Ciafaloni, Phys. Lett. B **412**, 396 (1997) [Erratum-ibid. B **417**, 390 (1997)] [hep-ph/9707390];
Phys. Lett. B **430**, 349 (1998) [hep-ph/9803389].
- [6] Y. V. Kovchegov and A. H. Mueller, Phys. Lett. B **439**, 428 (1998) [hep-ph/9805208].
- [7] N. Armesto, J. Bartels and M. A. Braun, Phys. Lett. B **442**, 459 (1998) [hep-ph/9808340].
- [8] E. Levin, hep-ph/9806228.
- [9] M. Ciafaloni and D. Colferai, Phys. Lett. B **452**, 372 (1999) [hep-ph/9812366];
M. Ciafaloni, D. Colferai and G. P. Salam, Phys. Rev. D **60**, 114036 (1999) [hep-ph/9905566].

- [10] D. A. Ross, Phys. Lett. B **431**, 161 (1998) [hep-ph/9804332].
- [11] R. D. Ball and S. Forte, hep-ph/9805315.
- [12] J. Blumlein and A. Vogt, Phys. Rev. D **58**, 014020 (1998) [hep-ph/9712546];
J. Blumlein, V. Ravindran, W. L. van Neerven and A. Vogt, hep-ph/9806368.
- [13] S. J. Brodsky, V. S. Fadin, V. T. Kim, L. N. Lipatov and G. B. Pivovarov, JETP Lett. **70**, 155 (1999) [hep-ph/9901229].
- [14] S. J. Brodsky, G. P. Lepage and P. B. Mackenzie, Phys. Rev. D **28**, 228 (1983).
- [15] B. Andersson, G. Gustafson and J. Samuelsson, Nucl. Phys. B **467**, 443 (1996).
- [16] L.N. Lipatov, talk presented at the 4th Workshop on Small- x and Diffractive Physics, Fermi National Accelerator Laboratory, Sept. 17-20, 1998.
- [17] G. P. Salam, JHEP **9807**, 019 (1998) [hep-ph/9806482].
- [18] Y. L. Dokshitzer, Sov. Phys. JETP **46**, 641 (1977) [Zh. Eksp. Teor. Fiz. **73**, 1216 (1977)];
V. N. Gribov and L. N. Lipatov, Yad. Fiz. **15**, 781 (1972) [Sov. J. Nucl. Phys. **15**, 438 (1972)];
G. Altarelli and G. Parisi, Nucl. Phys. B **126**, 298 (1977).
- [19] G. P. Salam, Acta Phys. Polon. B **30**, 3679 (1999) [hep-ph/9910492].
- [20] G. Altarelli, R. D. Ball and S. Forte, Nucl. Phys. B **575**, 313 (2000) [hep-ph/9911273];
G. Altarelli, R. D. Ball and S. Forte, Nucl. Phys. B **599**, 383 (2001) [hep-ph/0011270].
- [21] J. R. Forshaw, D. A. Ross and A. Sabio Vera, Phys. Lett. B **455**, 273 (1999) [hep-ph/9903390].
- [22] V. Del Duca and C. R. Schmidt, Phys. Rev. D **49**, 4510 (1994) [hep-ph/9311290].
- [23] W. J. Stirling, Nucl. Phys. B **423**, 56 (1994) [hep-ph/9401266].
- [24] V. Del Duca and C. R. Schmidt, Phys. Rev. D **51**, 2150 (1995) [hep-ph/9407359].
- [25] C. R. Schmidt, Phys. Rev. Lett. **78**, 4531 (1997) [hep-ph/9612454].
- [26] L. H. Orr and W. J. Stirling, Phys. Rev. D **56**, 5875 (1997) [hep-ph/9706529].

- [27] B. Abbott *et al.* [D0 Collaboration], FERMILAB-CONF-97-371-E *Contributed to 18th International Symposium on Lepton - Photon Interactions (LP 97), Hamburg, Germany, 28 Jul - 1 Aug 1997, and Contributed to International Europhysics Conference on High-Energy Physics (HEP 97), Jerusalem, Israel, 19-26 Aug 1997*;
S. Abachi *et al.* [D0 Collaboration], Phys. Rev. Lett. **77**, 595 (1996) [hep-ex/9603010].
- [28] A. H. Mueller and H. Navelet, Nucl. Phys. B **282**, 727 (1987).
- [29] B. Abbott *et al.* [D0 Collaboration], Phys. Rev. Lett. **84**, 5722 (2000) [hep-ex/9912032].
- [30] J. R. Andersen, V. Del Duca, S. Frixione, C. R. Schmidt and W. J. Stirling, JHEP **0102**, 007 (2001) [hep-ph/0101180].
- [31] A. Mueller, Nucl. Phys. B (Proc. Suppl.) **18C**, 125 (1991).
- [32] J. Kwiecinski, A. D. Martin and P. J. Sutton, Phys. Rev. D **46**, 921 (1992);
J. Bartels, A. de Roeck and M. Loewe, Z. Phys. C **54**, 635 (1992);
W. Tang, Phys. Lett. B **278**, 363 (1992).
- [33] C. Adloff *et al.* [H1 Collaboration], Nucl. Phys. B **538**, 3 (1999) [hep-ex/9809028].
- [34] J. Breitweg *et al.* [ZEUS Collaboration], Eur. Phys. J. C **6**, 239 (1999) [hep-ex/9805016].
- [35] L. Lonnblad, Comput. Phys. Commun. **71**, 15 (1992).
- [36] H. Jung, Comput. Phys. Commun. **86**, 147 (1995). H. Jung, L. Jonsson and H. Kuster, Eur. Phys. J. C **9**, 383 (1999) [hep-ph/9903306].
- [37] J. Bartels, V. Del Duca, A. De Roeck, D. Graudenz and M. Wusthoff, Phys. Lett. B **384**, 300 (1996) [hep-ph/9604272].
- [38] S. Catani and M. H. Seymour, Phys. Lett. B **378**, 287 (1996) [hep-ph/9602277].
S. Catani and M. H. Seymour, Nucl. Phys. B **485**, 291 (1997) [Erratum-ibid. B **510**, 503 (1997)] [hep-ph/9605323].
- [39] E. Mirkes and D. Zeppenfeld, Phys. Rev. Lett. **78**, 428 (1997) [hep-ph/9609231].
- [40] J. G. Contreras, R. Peschanski and C. Royon, Phys. Rev. D **62**, 034006 (2000) [hep-ph/0002057];
J. G. Contreras, Phys. Lett. B **446**, 158 (1999) [hep-ph/9812255].

- [41] J. Kwiecinski, A. D. Martin and J. J. Outhwaite, Eur. Phys. J. C **9**, 611 (1999) [hep-ph/9903439].
- [42] H. Jung and G. P. Salam, Eur. Phys. J. C **19**, 351 (2001) [hep-ph/0012143].
- [43] M. Ciafaloni, Nucl. Phys. B **296**, 49 (1988);
S. Catani, F. Fiorani and G. Marchesini, Phys. Lett. B **234**, 339 (1990);
S. Catani, F. Fiorani and G. Marchesini, Nucl. Phys. B **336**, 18 (1990).
- [44] G. Kramer and B. Potter, Phys. Lett. B **453**, 295 (1999) [hep-ph/9901314].
- [45] J. Bartels, A. De Roeck and H. Lotter, Phys. Lett. B **389**, 742 (1996) [hep-ph/9608401];
S. J. Brodsky, F. Hautmann and D. E. Soper, Phys. Rev. D **56**, 6957 (1997) [hep-ph/9706427].
- [46] M. Acciarri *et al.* [L3 Collaboration], Phys. Lett. B **453**, 333 (1999).
- [47] L3 Collaboration, L3 Note 2568, presented at ICHEP 2000, Osaka, Japan.
- [48] OPAL Collaboration, OPAL Physics Notes PN456.
- [49] M. Cacciari, V. Del Duca, S. Frixione and Z. Trocsanyi, JHEP **0102**, 029 (2001) [hep-ph/0011368].